

# Quarkonium Recombination In Presence of Strangeness Rich Expanding QGP

BNL, December 14, 2005

With: Jean Letessier, and Inga Kouznetsova

## OBJECTIVES:

1. Understanding the strangeness RHIC results;
2. Dynamics of thermal  $s$  and  $c$  production at RHIC-200 (and extrapolate to LHC);
3. Strangeness/expansion impact on redistribution of charm/bottom into hadrons.

**ABSTRACT:** Kinetic strangeness production is compared to the available strangeness yield measurements at RHIC. QGP yield saturation as function of initial conditions and evolution scenarios are considered. Insights gained allow to narrow down the expectations for strangeness production at LHC and to evaluate thermal charm production yields at RHIC and LHC. Implications for yields of Charmonium,  $D_s$  meson, and  $B_c$  will be presented.

---

*Supported by a grant from the U.S. Department of Energy, DE-FG02-04ER41318*

*Johann Rafelski  
Department of Physics  
University of Arizona  
TUCSON, AZ, USA*

# CONTENTS

1. Chemical Non-equilibrium
2. Statistical Hadronization
3. Fits to Particle Yields: RHIC-200
4. QCD Predicts Strangeness Yield: RHIC and LHC
5. Implications for Charm at RHIC and LHC
6. Conclusions

•

# 1. Chemical Non-equilibrium

## INPUT: (Valence) Quark-Yield in Chemical Non-equilibrium

MOTIVATION: QGP fireball subject to rapid expansion, **expect chemical nonequilibrium.** “So What”?

- Shift in hadron yields between a) baryons and mesons; and b) strange and non-strange quarks;
- Strangeness signature of deconfinement
- Chemical non-equilibrium quark ‘occupancy’ can **favor** / **disfavor** presence of a phase transition. **What  $\mu_B$  can do,  $\gamma_i$  can do better as both quark and antiquark number increase/decrease together.**
- **At LHC Strangeness yield chemistry alters yields of CHARMED HADRONS;**

### REMINDER:

$\mu_b$  controls the particle difference = baryon number.

$\gamma_i$  regulates the number of particle-antiparticle pairs present.

DISTINGUISH: **HG** and **QGP parameters:** micro-canonical variables such as baryon number, strangeness, charm, bottom, etc flavors are continuous and entropy is almost continuous across any phase boundary encountered in HI collisions, even in presence of a rapid change in **STRUCTURE** of the phase.

THEREFORE:  $\gamma_i$  will in general be **discontinuous:** e.g.  $\gamma_s^{\text{QGP}} \neq \gamma_s^{\text{HG}}$ . However,  $\mu_i$  are **continuous**, with the proviso that by definition  $3\mu_q = \mu_B$ ,  $\mu_s = \mu_B/3 - \mu_S$ .

## Mathematical Need for Non-Equilibrium Parameters

- $\tilde{\gamma}_s \equiv \gamma_s/\gamma_q$  shifts the yield of strange vs non-strange hadrons:

$$\frac{K^+}{\pi^+} \propto \frac{\gamma_s}{\gamma_q}, \quad \frac{\phi}{h} \propto \frac{\gamma_s^2}{\gamma_q^2}, \quad \frac{\Omega}{\Lambda} \propto \frac{\gamma_s^2}{\gamma_q^2},$$

- For fixed  $\tilde{\gamma}_s \equiv \gamma_s/\gamma_q$  and fixed other statistical parameters ( $T, \lambda_i, \dots$ ):

$$\frac{\text{baryons}}{\text{mesons}} \propto \frac{\gamma_q^3}{\gamma_q^2} = \gamma_q.$$

**NOTE: across any phase boundary**

$$\gamma_s^{\text{QGP}} \neq \gamma_s^{\text{HG}} \quad \gamma_q^{\text{QGP}} \neq \gamma_q^{\text{HG}}$$

**Smooth across the phase boundary are the observable yields  
strangeness, charm, entropy = multiplicity  
and in particular the volume independent observables:**

$$\frac{s \text{ or } c}{S} = \frac{\text{number of valance strange, charm quark pairs}}{\text{multiplicity} = \text{entropy content in final state}}$$

**Our kinetic approach depends on these ‘micro-canonical’ variables,  
 $\gamma_i$  are entirely auxiliary.**

## Strangeness / Entropy

Relative  $s/S$  yield measures the number of active degrees of freedom and degree of relaxation when strangeness production freezes-out. Perturbative expression in chemical equilibrium:

$$\frac{s}{S} = \frac{\frac{g_s}{2\pi^2} T^3 (m_s/T)^2 K_2(m_s/T)}{(g_2\pi^2/45)T^3 + (g_s n_f/6)\mu_q^2 T} \simeq 0.028$$

much of  $\mathcal{O}(\alpha_s)$  interaction effect cancels out

Allow for chemical non-equilibrium of strangeness  $\gamma_s^{\text{QGP}}$ , and possible quark-gluon pre-equilibrium – gradual increase to the limit expected:

$$\frac{s}{S} = \frac{0.03\gamma_s^{\text{QGP}}}{0.4\gamma_G + 0.1\gamma_s^{\text{QGP}} + 0.5\gamma_q^{\text{QGP}} + 0.05\gamma_q^{\text{QGP}}(\ln \lambda_q)^2} \rightarrow 0.028.$$

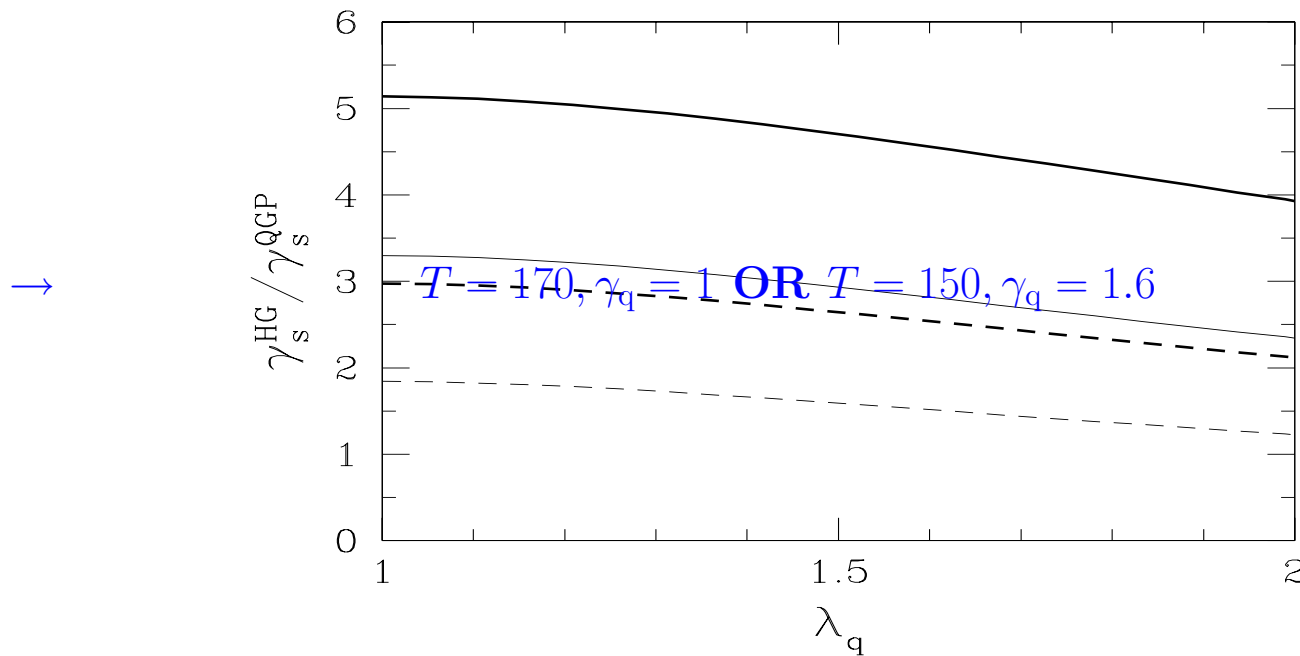
We expect the yield of gluons and light quarks to approach chemical equilibrium fast and first:  $\gamma_G \rightarrow 1$  and  $\gamma_q^{\text{QGP}} \rightarrow 1$ , thus  $s/S \simeq 0.028\gamma_s^{\text{QGP}}$ .

**CHECK: FIT YIELDS OF PARTICLES, EVALUATE STRANGENESS AND ENTROPY CONTENT AND COMPARE WITH EXPECTED RATIO,**

$$\gamma_i^{\text{HG}} > \gamma_i^{\text{QGP}}; \text{ EXPECTED INCREASE QGP} \rightarrow \text{HG}$$

In fast breakup of expanding QGP,  $V^{\text{HG}} \simeq V^{\text{QGP}}$ ,  $T^{\text{QGP}} \simeq T^{\text{HG}}$ , the chemical occupancy factors accommodate the different magnitude of particle phase space. Chemical equilibrium in one phase means non-equilibrium in the the other.

Compare phase spaces to obtain  $\gamma_s^{\text{HG}} / \gamma_s^{\text{QGP}}$



$\gamma_s^{\text{HG}} / \gamma_s^{\text{QGP}}$  Solid lines  $\gamma_q^{\text{HG}} = 1$ ,

Probably appropriate: short dashed  $\gamma_q^{\text{HG}} = 1.6$ .

Thin lines for  $T = 170$  and thick lines  $T = 150$  MeV, common to both phases.

$$\gamma_s^{\text{HG}} \simeq 2 - 4 \gamma_s^{\text{QGP}}$$

When we fix  $s/S$  (strangeness/entropy), see below, factor follows exactly.

# HIGH ENTROPY STATE AND THE EXPECTED $\gamma_q^{\text{HG}}$

QGP has excess of entropy, maximize entropy density at hadronization:

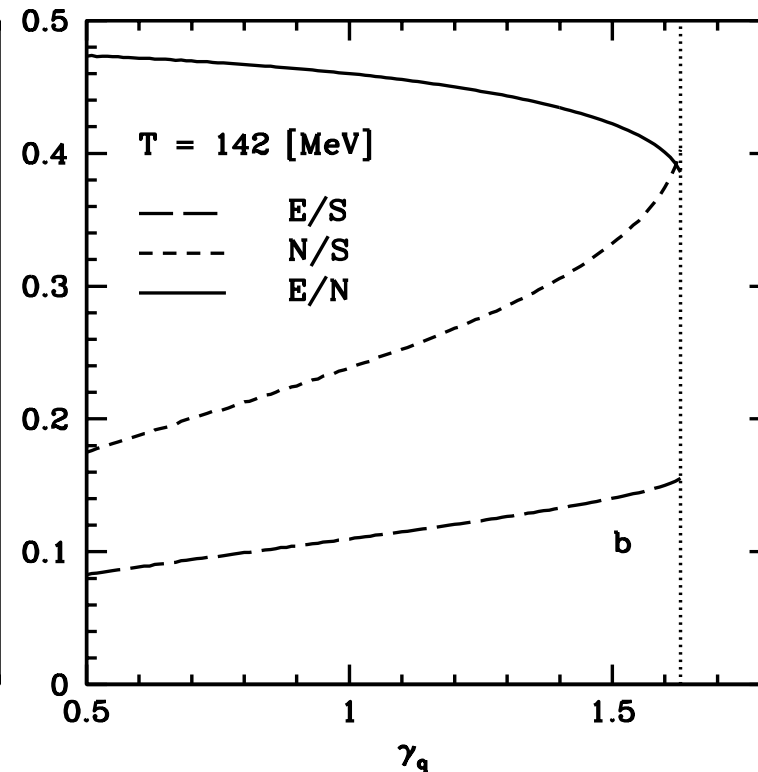
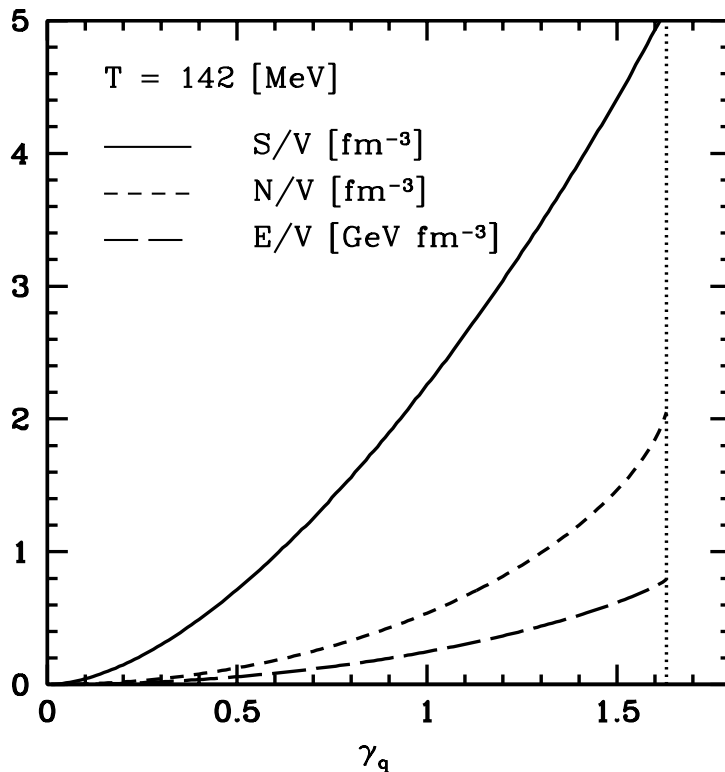
$$\gamma_q^2 \rightarrow e^{m_\pi/T} :$$

Example: maximization of entropy density in pion gas

$$E_\pi = \sqrt{m_\pi^2 + p^2}$$

$$S_{B,F} = \int \frac{d^3p d^3x}{(2\pi\hbar)^3} [\pm(1 \pm f) \ln(1 \pm f) - f \ln f] , \quad f_\pi(E) = \frac{1}{\gamma_q^{-2} e^{E_\pi/T} - 1} .$$

Pion gas properties:  
*N*-particle,  
*E*-energy,  
*S*-entropy,  
*V*-volume  
as function  
of  $\gamma_q$ .



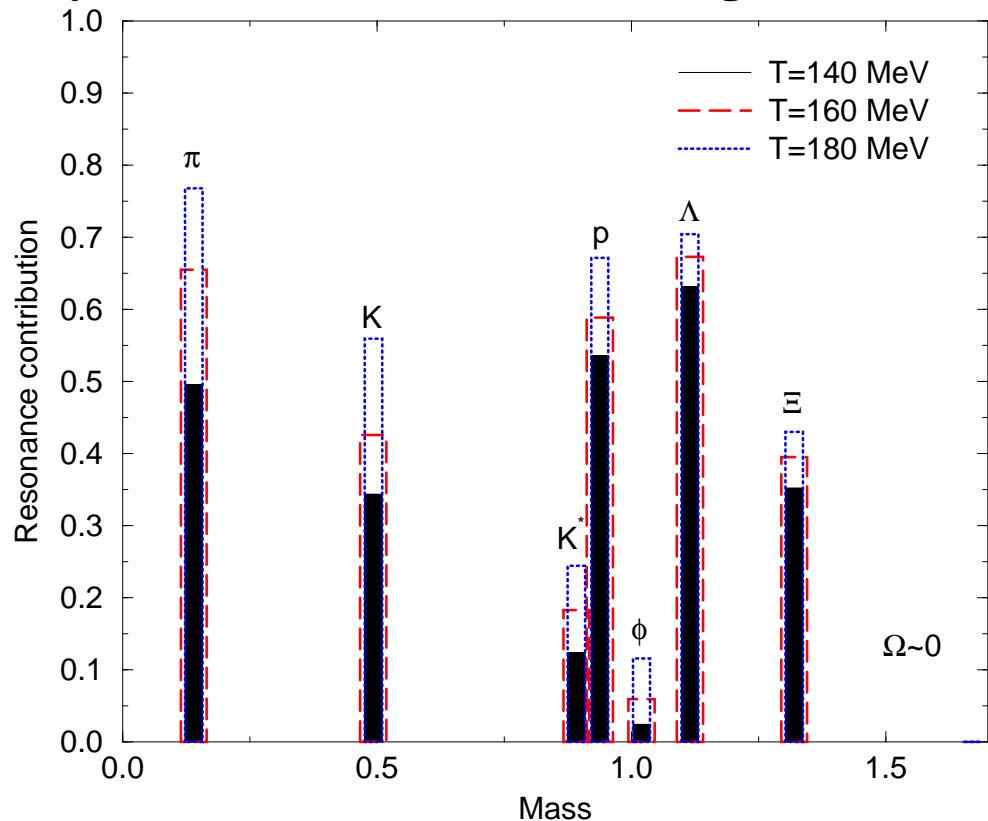
•

## 2. Statistical Hadronization

Hypothesis (Fermi, Hagedorn): particle production can be described by evaluating the accessible phase space.

## Verification of statistical hadronization:

Particle yields with same valance quark content are in relative chemical equilibrium, e.g. the relative yield of  $\Delta(1230)/N$  as of  $K^*/K$ ,  $\Sigma^*(1385)/\Lambda$ , etc, is controlled by chemical freeze-out i.e. Hagedorn Temperature  $T_H$ :



$$\frac{N^*}{N} = \frac{g^*(m^*T_H)^{3/2} e^{-m^*/T_H}}{g(mT_H)^{3/2} e^{-m/T_H}}$$

Resonances decay rapidly into ‘stable’ hadrons and dominate the yield of most stable hadronic particles.

Resonance yields test statistical hadronization principles.

Resonances reconstructed by invariant mass; important to consider potential for loss of observability.

**HADRONIZATION GLOBAL FIT: →**

## Counting particles

The counting of hadrons is conveniently done by counting the valence quark content ( $u, d, s, \dots \lambda_q^2 = \lambda_u \lambda_d, \lambda_{I3} = \lambda_u / \lambda_d$ ) :

$$\Upsilon_i \equiv \prod_i \gamma_i^{n_i} \lambda_i^{k_i} = e^{\sigma_i/T}; \quad \lambda_q \equiv e^{\frac{\mu_q}{T}} = e^{\frac{\mu_b}{3T}}, \quad \lambda_s \equiv e^{\frac{\mu_s}{T}} = e^{\frac{[\mu_b/3 - \mu_S]}{T}}$$

**Example of NUCLEONS**  $\gamma_N = \gamma_q^3$ :

$$\Upsilon_N = \gamma_N e^{\frac{\mu_b}{T}}, \quad \Upsilon_{\bar{N}} = \gamma_N e^{\frac{-\mu_b}{T}};$$

$$\sigma_N \equiv \mu_b + T \ln \gamma_N, \quad \sigma_{\bar{N}} \equiv -\mu_b + T \ln \gamma_N$$

Meaning of parameters from e.g. the first law of thermodynamics:

$$\begin{aligned} dE + P dV - T dS &= \sigma_N dN + \sigma_{\bar{N}} d\bar{N} \\ &= \mu_b (dN - d\bar{N}) + T \ln \gamma_N (dN + d\bar{N}). \end{aligned}$$

**NOTE:** For  $\gamma_N \rightarrow 1$  the pair terms vanishes, the  $\mu_b$  term remains, it costs  $dE = \mu_B$  to add to baryon number.

## Statistical Hadronization fits of hadron yields

Full analysis of experimental hadron yield results requires a significant numerical effort in order to allow for resonances, particle widths, full decay trees, isospin multiplet sub-states.

**Kraków-Tucson NATO supported collaboration** produced a public package **SHARE Statistical Hadronization with Resonances** which is available e.g. at

<http://www.physics.arizona.edu/~torrieri/SHARE/share.html>

Lead author: **Giorgio Torrieri**

With W. Broniowski, W. Florkowski, J. Letessier, S. Steinke, JR  
nucl-th/0404083 *Comp. Phys. Com.* 167, 229 (2005)

**Online SHARE:** Steve Steinke No fitting online (server too small)

<http://www.physics.arizona.edu/~steinke/shareonline.html>

**Aside of particle yields, also PHYSICAL PROPERTIES** of the source are available, both in SHARE and ONLINE.

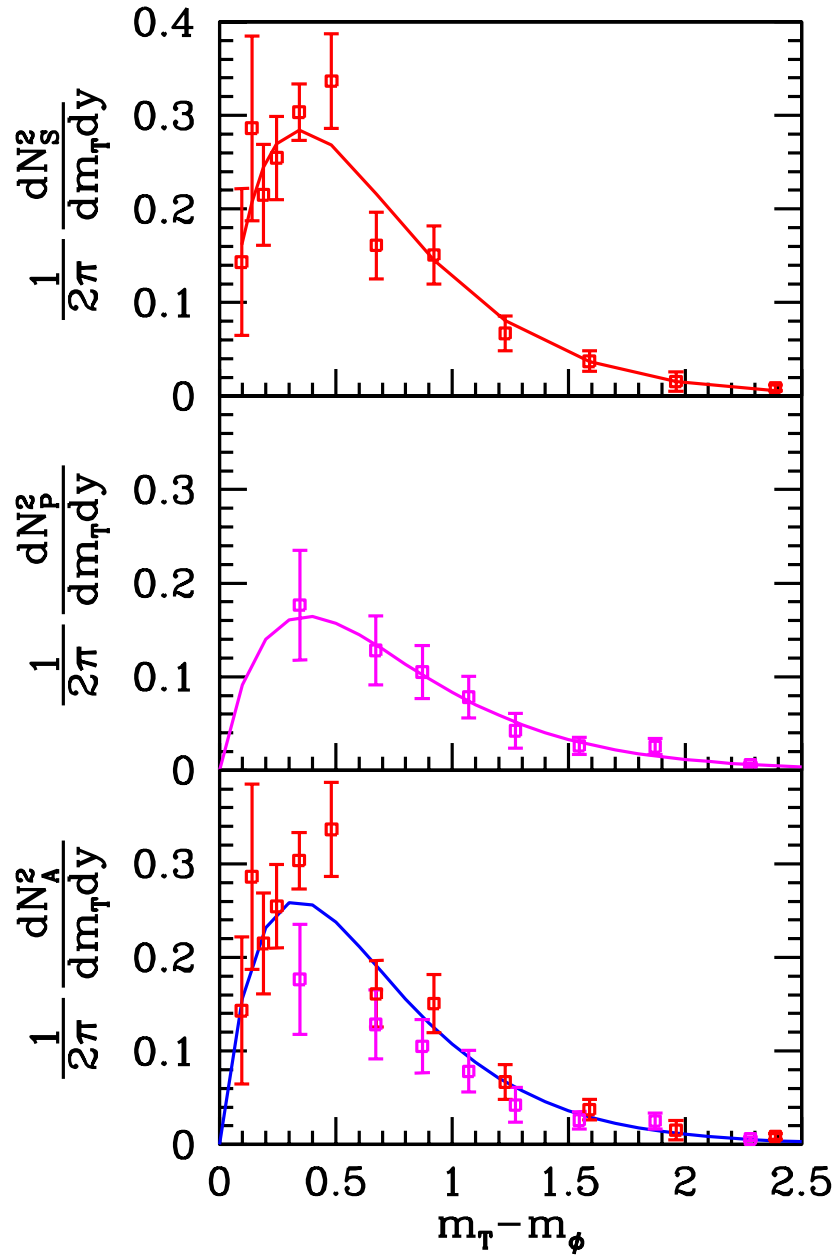
•

### **3. Fits to Particle Yields: RHIC-200**

**Example we need: Fit of RHIC-200 as function of centrality, mostly non-strange hadrons. Implicit ab-initio prediction of strange and multistrange hadrons.**

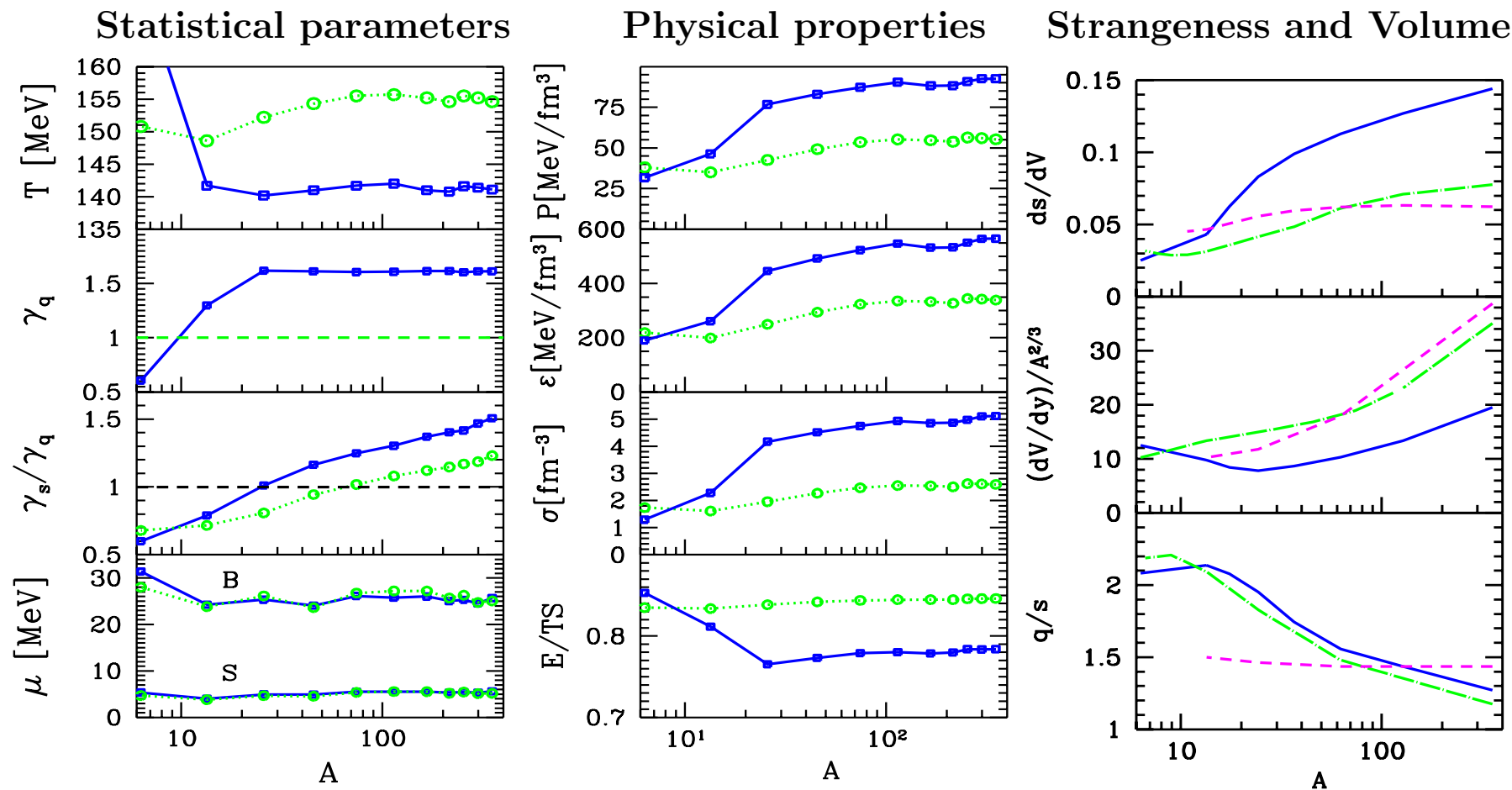
**DATA: Centrality dependence of  $dN/dy$  for  $\pi^\pm$ ,  $K^\pm$ ,  $p$  and  $\bar{p}$ . The errors are systematic only. The statistical errors are negligible. PHENIX data**

$N_{part}$	$\pi^+$	$\pi^-$	$K^+$	$K^-$	$p$	$\bar{p}$
351.4	286.4 $\pm$ 24.2	281.8 $\pm$ 22.8	48.9 $\pm$ 6.3	45.7 $\pm$ 5.2	18.4 $\pm$ 2.6	13.5 $\pm$ 1.8
299.0	239.6 $\pm$ 20.5	238.9 $\pm$ 19.8	40.1 $\pm$ 5.1	37.8 $\pm$ 4.3	15.3 $\pm$ 2.1	11.4 $\pm$ 1.5
253.9	204.6 $\pm$ 18.0	198.2 $\pm$ 16.7	33.7 $\pm$ 4.3	31.1 $\pm$ 3.5	12.8 $\pm$ 1.8	9.5 $\pm$ 1.3
215.3	173.8 $\pm$ 15.6	167.4 $\pm$ 14.4	27.9 $\pm$ 3.6	25.8 $\pm$ 2.9	10.6 $\pm$ 1.5	7.9 $\pm$ 1.1
166.6	130.3 $\pm$ 12.4	127.3 $\pm$ 11.6	20.6 $\pm$ 2.6	19.1 $\pm$ 2.2	8.1 $\pm$ 1.1	5.9 $\pm$ 0.8
114.2	87.0 $\pm$ 8.6	84.4 $\pm$ 8.0	13.2 $\pm$ 1.7	12.3 $\pm$ 1.4	5.3 $\pm$ 0.7	3.9 $\pm$ 0.5
74.4	54.9 $\pm$ 5.6	52.9 $\pm$ 5.2	8.0 $\pm$ 0.8	7.4 $\pm$ 0.6	3.2 $\pm$ 0.5	2.4 $\pm$ 0.3
45.5	32.4 $\pm$ 3.4	31.3 $\pm$ 3.1	4.5 $\pm$ 0.4	4.1 $\pm$ 0.4	1.8 $\pm$ 0.3	1.4 $\pm$ 0.2
25.7	17.0 $\pm$ 1.8	16.3 $\pm$ 1.6	2.2 $\pm$ 0.2	2.0 $\pm$ 0.1	0.93 $\pm$ 0.15	0.71 $\pm$ 0.12
13.4	7.9 $\pm$ 0.8	7.7 $\pm$ 0.7	0.89 $\pm$ 0.09	0.88 $\pm$ 0.09	0.40 $\pm$ 0.07	0.29 $\pm$ 0.05
6.3	4.0 $\pm$ 0.4	3.9 $\pm$ 0.3	0.44 $\pm$ 0.04	0.42 $\pm$ 0.04	0.21 $\pm$ 0.04	0.15 $\pm$ 0.02



Include STAR data on  $K^*(892)/K^-$ , and  $\phi/K^-$  relative yields, these help decisively fix  $\gamma_s$  ( $\phi \propto \gamma_s^2$ ) and  $T : Y \propto m^{3/2} e^{-m/T}$  for  $m \gg T$ .

We considered the difference between STAR and PHENIX  $\phi$  yields. The lines show our best fit results to STAR (top panel), PHENIX (middle panel) and combined data set (bottom panel). The integrated yields agree for the top two panels with those reported by the experimental collaborations. We note that the integrated yield derived from the combined data fit (bottom panel), to all available 10% centrality  $\phi$ -yields, is not compatible with the PHENIX yield. This is so, since the evaluation of the integrated PHENIX  $\phi$ -yield depends on the lowest  $m_\perp$  measured yield. This data point appears to be a 1.5 s.d. low anomaly compared to the many STAR  $\phi$ -results available at low  $m_\perp$ . This possibly statistical fluctuation materially influences the total integrated PHENIX  $\phi$ -yield.

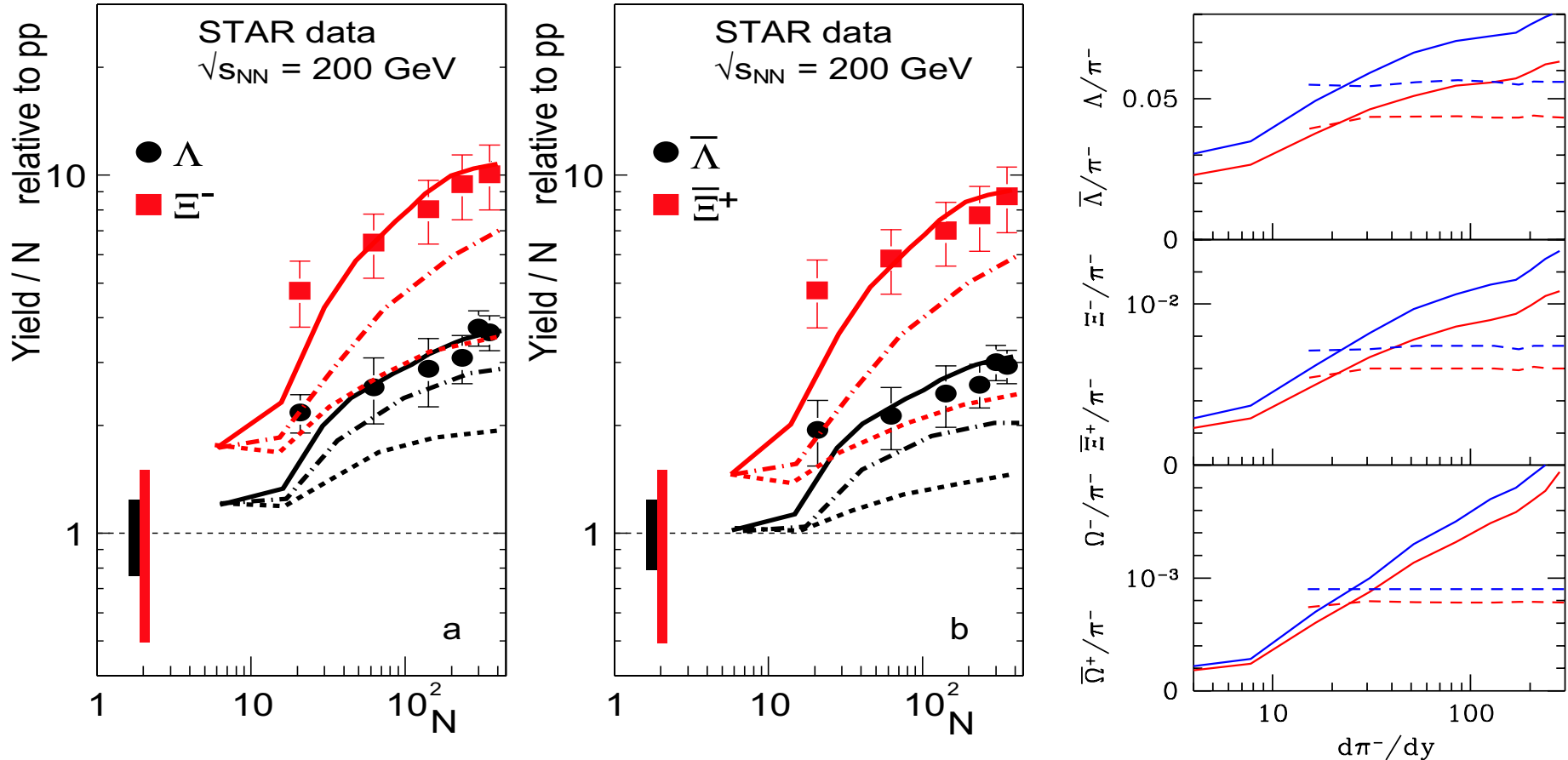


**LINES:**  $\gamma_s, \gamma_q \neq 1$  and  $\gamma_s \neq 1, \gamma_q = 1$ , also  $\gamma_s = \gamma_q = 1$   
 $\gamma_q$  changes with  $A \propto V$  from under-saturated to over-saturated value,  $\gamma_s^{\text{HG}}$  increases steadily to 2.4, implying near saturation in QGP.  $P, \sigma, \epsilon$  increase by factor 2–3, at  $A > 20$  (onset of new physics?),  $E/TS$  decreases with  $A$ .

Statistical + fit errors are seen in fluctuations, systematic error impacts absolute normalization by  $\pm 10\%$ .

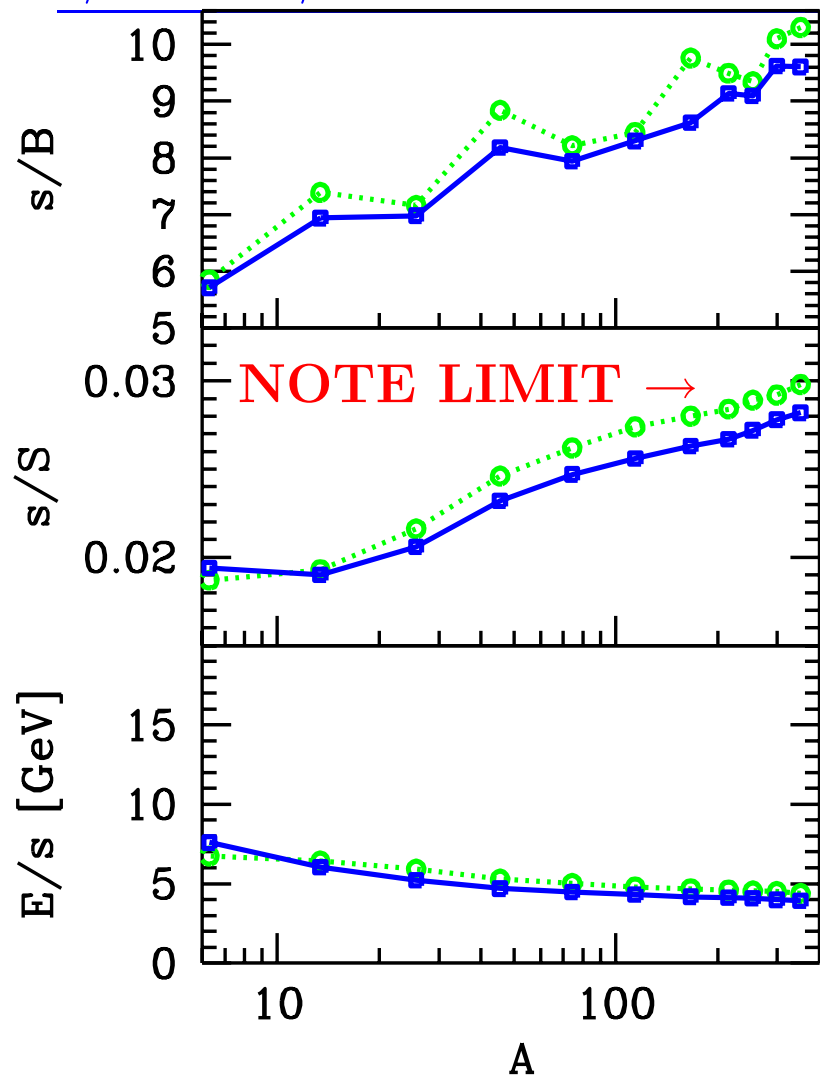
## RHIC200 PREDICTION OF dependence on centrality

Changes in REFERENCE yields which define 1 do not alter Th/Ex-agreement



STAR  $\sqrt{s_{NN}} = 200$  GeV yields of hyperons  $d\Lambda/dy$  and  $d\Xi^-/dy$ , (a), and antihyperons  $d\bar{\Lambda}/dy$  and  $d\bar{\Xi}^+/dy$ , (b), normalized with, and as function of,  $A$ , relative to these yields in  $pp$  reactions:  $d(\Lambda + \bar{\Lambda})/dy = 0.066 \pm 0.006$ ,  $d(\Xi^- + \bar{\Xi}^+)/dy = 0.0036 \pm 0.0012$ ,  $\bar{\Lambda}/\Lambda = 0.88 \pm 0.09$  and  $\bar{\Xi}^+/\Xi^- = 0.90 \pm 0.09$ . **Solid lines, chemical non-equilibrium, dashed chemical equilibrium, gry (dash-dotted lines, semi-equilibrium. )** On right, the predicted hyperons per  $\pi^-$  yields (blue for hyperons and **for antihyperons**).

$s/b$  and  $s/S$  rise with increasing centrality  $A \propto V$ ;  $E/s$  falls



Showing results for both  $\gamma_q, \gamma_s \neq 1$ , for  $\gamma_s \neq 1, \gamma_q = 1$ . Note little difference in the result, even though the value of  $T$  will differ significantly.

- 1)  $s/S \rightarrow 0.027$ , as function of  $V$ ;
- 2) most central value near QGP chemical equilibrium;
- 3) no saturation for largest volumes available;

Behavior is consistent with QGP prediction of steady increase of strangeness yield with increase of the volume, which implies longer lifespan and hence greater strangeness yield, both specific yield and larger  $\gamma_s^{\text{QGP}}$ .

Agreement between nonequilibrium (blue) and semi-equilibrium (green,  $\gamma_q = 1$ ) in description of bulk properties implies that MOST particle distributions extrapolate well from the experimental data - differences in e.g.  $\Omega, \bar{\Omega}$  yields sensitive to the model issues do not impact bulk properties decisively.

•

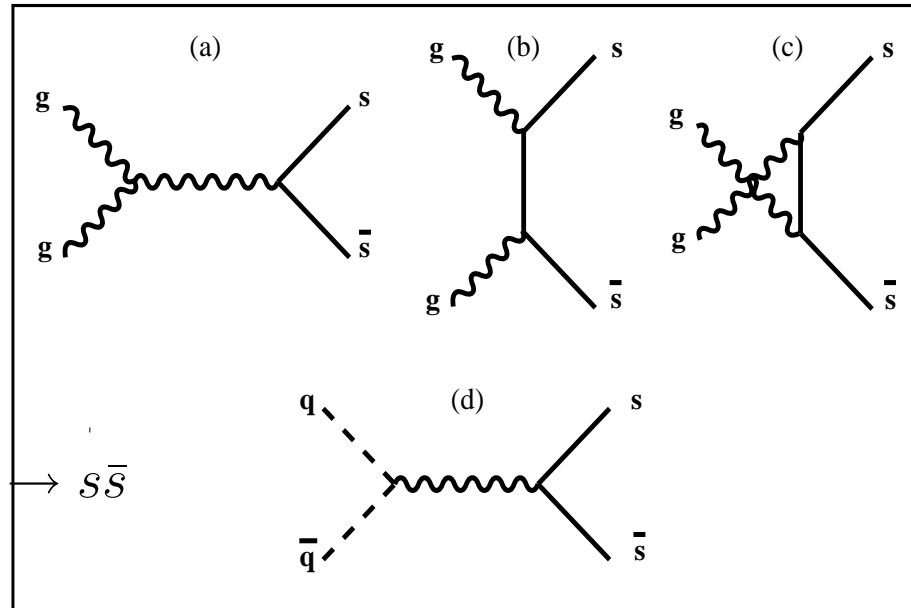
## **4. QCD Predicts Strangeness Yield: RHIC and LHC**

**COMPUTE and FINETUNE  $\gamma_s^{\text{QGP}}$  at RHIC - extrapolate  $\rightarrow$  LHC:**

- production of strangeness in gluon fusion  $GG \rightarrow s\bar{s}$   
strangeness linked to gluons from QGP;

dominant processes:  
 $GG \rightarrow s\bar{s}$   
abundant strangeness  
=evidence for gluons

10–15% of total rate:  $q\bar{q} \rightarrow s\bar{s}$



- coincidence of scales:

$$m_s \simeq T_c \rightarrow \tau_s \simeq \tau_{\text{QGP}} \rightarrow$$

strangeness a clock for QGP phase

- $\bar{s} \simeq \bar{q} \rightarrow$  strange antibaryon enhancement  
at RHIC (anti)hyperon dominance of (anti)baryons.

## Strangeness relaxation to chemical equilibrium

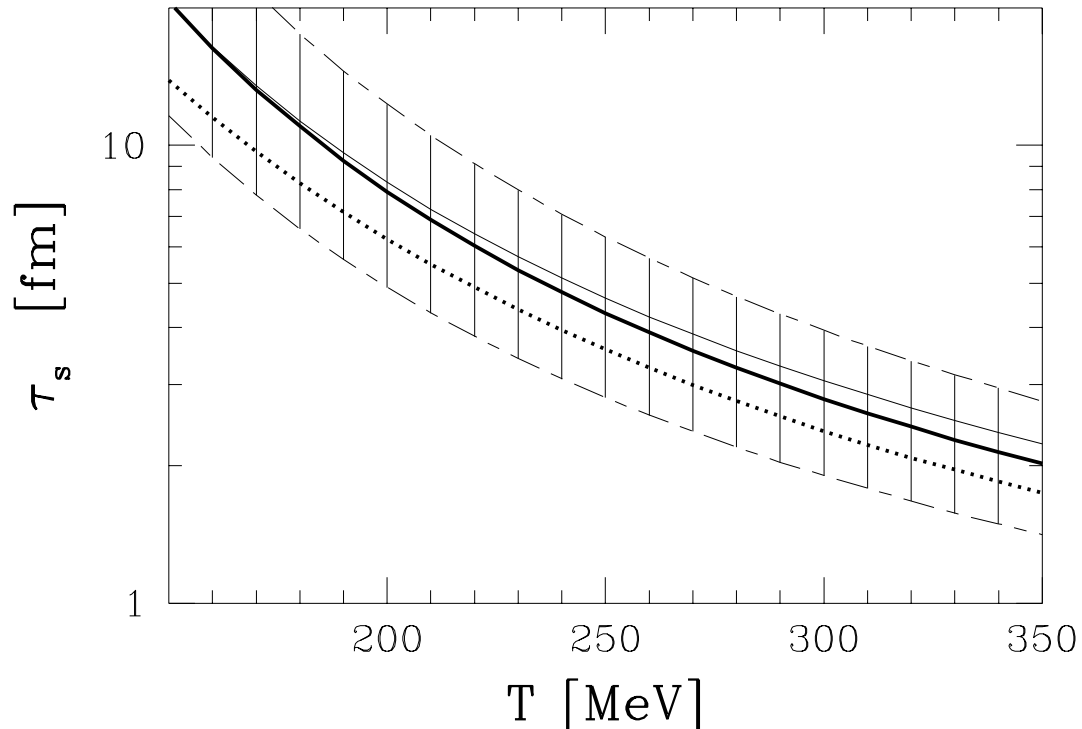
Strangeness density time evolution in local rest frame:

$$\frac{1}{V} \frac{ds}{d\tau} = \frac{1}{V} \frac{d\bar{s}}{d\tau} = \frac{1}{2} \rho_g^2(t) \langle \sigma v \rangle_T^{gg \rightarrow s\bar{s}} + \rho_q(t) \rho_{\bar{q}}(t) \langle \sigma v \rangle_T^{q\bar{q} \rightarrow s\bar{s}} - \rho_s(t) \rho_{\bar{s}}(t) \langle \sigma v \rangle_T^{s\bar{s} \rightarrow gg, q\bar{q}}$$

Evolution for  $s$  and  $\bar{s}$  identical, which allows to set  $\rho_s(t) = \rho_{\bar{s}}(t)$ .

Note invariant production rate  $A$  and the characteristic time constant  $\tau_s$ :

$$A^{12 \rightarrow 34} \equiv \frac{1}{1+\delta_{1,2}} \gamma_1 \gamma_2 \rho_1^\infty \rho_2^\infty \langle \sigma_s v_{12} \rangle_T^{12 \rightarrow 34}. \quad 2\tau_s \equiv \frac{\rho_s(\infty)}{A^{gg \rightarrow s\bar{s}} + A^{q\bar{q} \rightarrow s\bar{s}} + \dots}$$



## Thermal average rate of strangeness production

Kinetic (momentum) equilibration is faster than chemical, use thermal particle distributions  $f(\vec{p}_1, T)$  to obtain average rate:

$$\langle \sigma v_{\text{rel}} \rangle_T \equiv \frac{\int d^3p_1 \int d^3p_2 \sigma_{12} v_{12} f(\vec{p}_1, T) f(\vec{p}_2, T)}{\int d^3p_1 \int d^3p_2 f(\vec{p}_1, T) f(\vec{p}_2, T)}.$$

The generic angle averaged cross sections for (heavy) flavor  $s, \bar{s}$  production processes  $g + g \rightarrow s + \bar{s}$  and  $q + \bar{q} \rightarrow s + \bar{s}$ , are:

$$\bar{\sigma}_{gg \rightarrow s\bar{s}}(s) = \frac{2\pi\alpha_s^2}{3s} \left[ \left( 1 + \frac{4m_s^2}{s} + \frac{m_s^4}{s^2} \right) \tanh^{-1} W(s) - \left( \frac{7}{8} + \frac{31m_s^2}{8s} \right) W(s) \right],$$

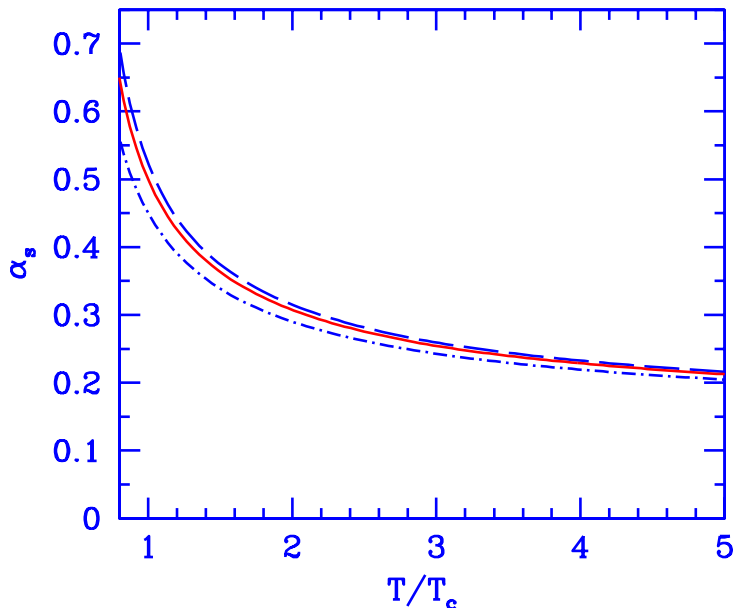
$$\bar{\sigma}_{q\bar{q} \rightarrow s\bar{s}}(s) = \frac{8\pi\alpha_s^2}{27s} \left( 1 + \frac{2m_s^2}{s} \right) W(s). \quad W(s) = \sqrt{1 - 4m_s^2/s}$$

### RESUMMATION

The relatively small experimental value  $\alpha_s(M_Z) \simeq 0.118$ , established in recent years helps to achieve QCD resummation with running  $\alpha_s$  and  $m_s$  taken at the energy scale  $\mu \equiv \sqrt{s}$ .  
Effective  $T$ -dependence:

$$\alpha_s(\mu = 2\pi T) \equiv \alpha_s(T) \simeq \frac{\alpha_s(T_c)}{1 + (0.760 \pm 0.002) \ln(T/T_c)}$$

with  $\alpha_s(T_c) = 0.50 \pm 0.04$  and  $T_c = 0.16$  GeV.  
 $\alpha_s^2$  varies by factor 10



## STRANGENESS IN ENTROPY CONSERVING EXPANSION

QGP expansion is adiabatic i.e. ( $g_G = 2_s \delta_c = 16, g_q = 2_s 3_c n_f$ )

$$S = \frac{4\pi^2}{90} g(T) V T^3 = \mathbf{Const.} \quad g = g_G \left( 1 - \frac{15\alpha_s(T)}{4\pi} + \dots \right) + \frac{7}{4} g_q \left( 1 - \frac{50\alpha_s(T)}{21\pi} + \dots \right) .$$

The volume, temperature change such that  $\delta(gT^3V) = 0$ . Strangeness phase space occupancy,  $g_s = 2_s 3_c \left( 1 - \frac{k\alpha_s(T)}{\pi} + \dots \right), k = 2$  for  $m_s/T \rightarrow 0$ :

$$\gamma_s(\tau) \equiv \frac{n_s(\tau)}{n_s^\infty(T(\tau))}, \quad n_s(\tau) = \gamma_s(\tau) T(\tau)^3 \frac{g_s(T)}{2\pi^2} z^2 K_2(z), \quad z = \frac{m_s}{T(t)}, \quad K_i : \text{Bessel f.}$$

evolves due to production and dilution, keeping **entropy** fixed:

$$\frac{d}{d\tau} \frac{s}{S} = \frac{A_G}{S/V} [\gamma_G^2 - \gamma_s^2] + \frac{A_q}{S/V} [\gamma_q^2 - \gamma_s^2]$$

Which for  $\gamma_s$  assumes the form that makes **dilution** explicit:

$$\frac{d\gamma_s}{d\tau} + \gamma_s \frac{d \ln[g_s z^2 K_2(z)/g]}{d\tau} = \frac{A_G}{n_s^\infty} [\gamma_G^2 - \gamma_s^2] + \frac{A_q}{n_s^\infty} [\gamma_q^2 - \gamma_s^2]$$

For  $m_s \rightarrow 0$  dilution effect decreases, disappears, and  $\gamma_s \leq \gamma_{G,q}$ , **importance** grows with mass of the quark,  $z = m_s(T)/T$ , which grows near phase transition boundary.

## Time evolution of $s/S$

To integrate the equation for  $s/S$  we need to understand  $T(\tau)$ .

We have at our disposal the final conditions:  $S(\tau_f)$ ,  $T(\tau_f)$  and since particle yields  $dN_i/dy = n_i dV/dy$  the volume per rapidity,  $\Delta V/\Delta y|_{\tau_f}$ . Theory (lattice) further provides Equations of State  $\sigma(T) = S/V$ . Hydrodynamic expansion with Bjørken scaling implies strictly  $dS/dy = \sigma(T)dV/dy = \text{Const.}$  as function of time.

$dV/dy(\tau)$  expansion completes the model.

$$\frac{dV}{dy} \propto A_{\perp}(\tau) dz/dy|_{\tau,y}$$

a) we need transverse area expansion,  $A_{\perp}(\tau)$ . We assume  $R_{\perp}(\tau) = R_0 + v_{\perp}(\tau)\tau$  and consider two geometries:

i)  $A_{\perp} = \pi R_{\perp}^2(\tau)$  bulk expansion

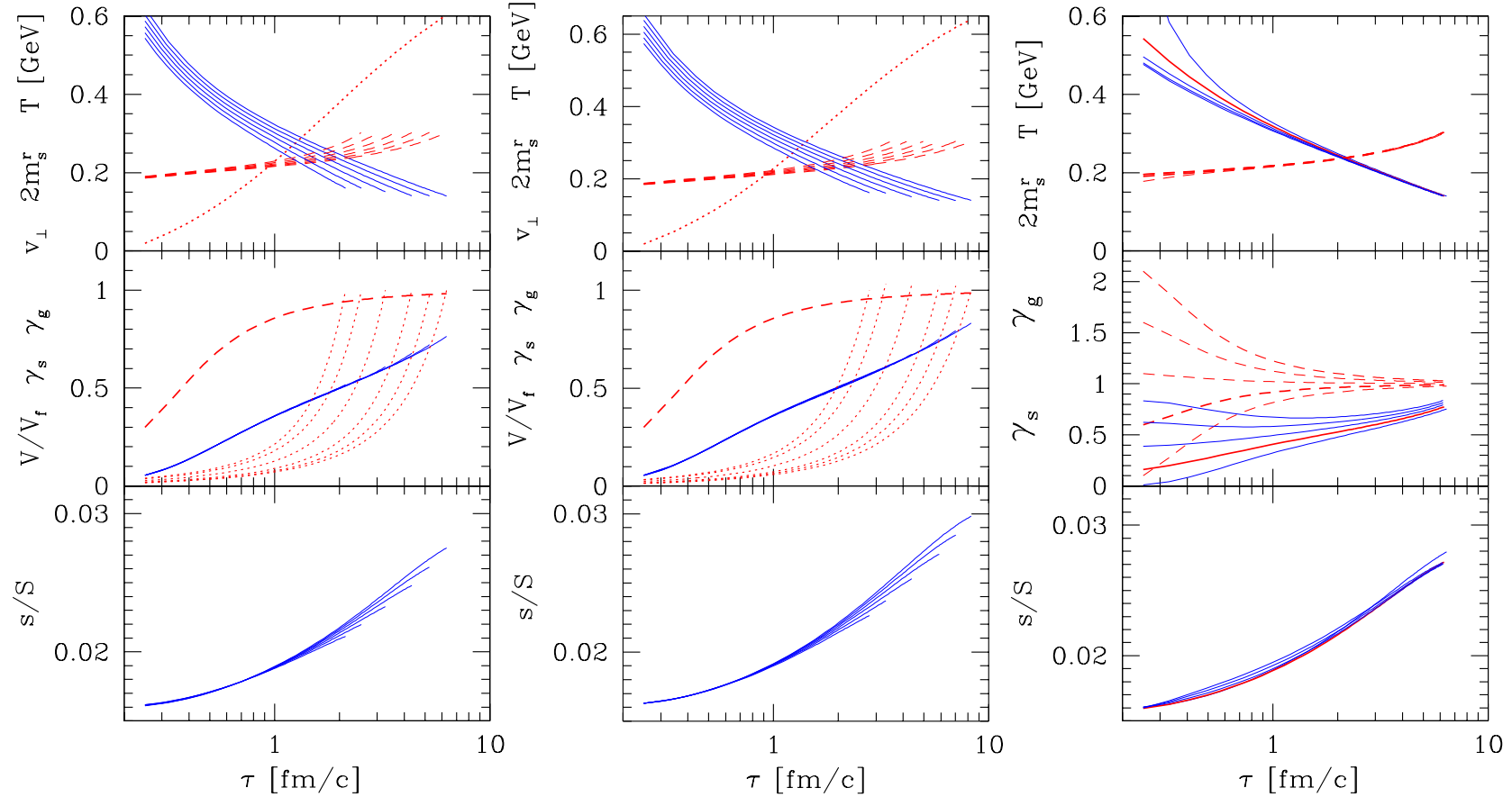
ii)  $A_{\perp} = \pi [R_{\perp}^2(\tau) - (R_{\perp}^2(\tau) - d)^2] = 2\pi d [R_{\perp}(\tau) - \frac{d}{2}]$  donut expansion and

b) we need to associate with the domain of observed rapidity  $\Delta y$  a geometric region at the source  $\Delta z$ . We take scaling Bjørken hydrodynamical solution:

$$\frac{dz}{dy} = \tau \cosh y.$$

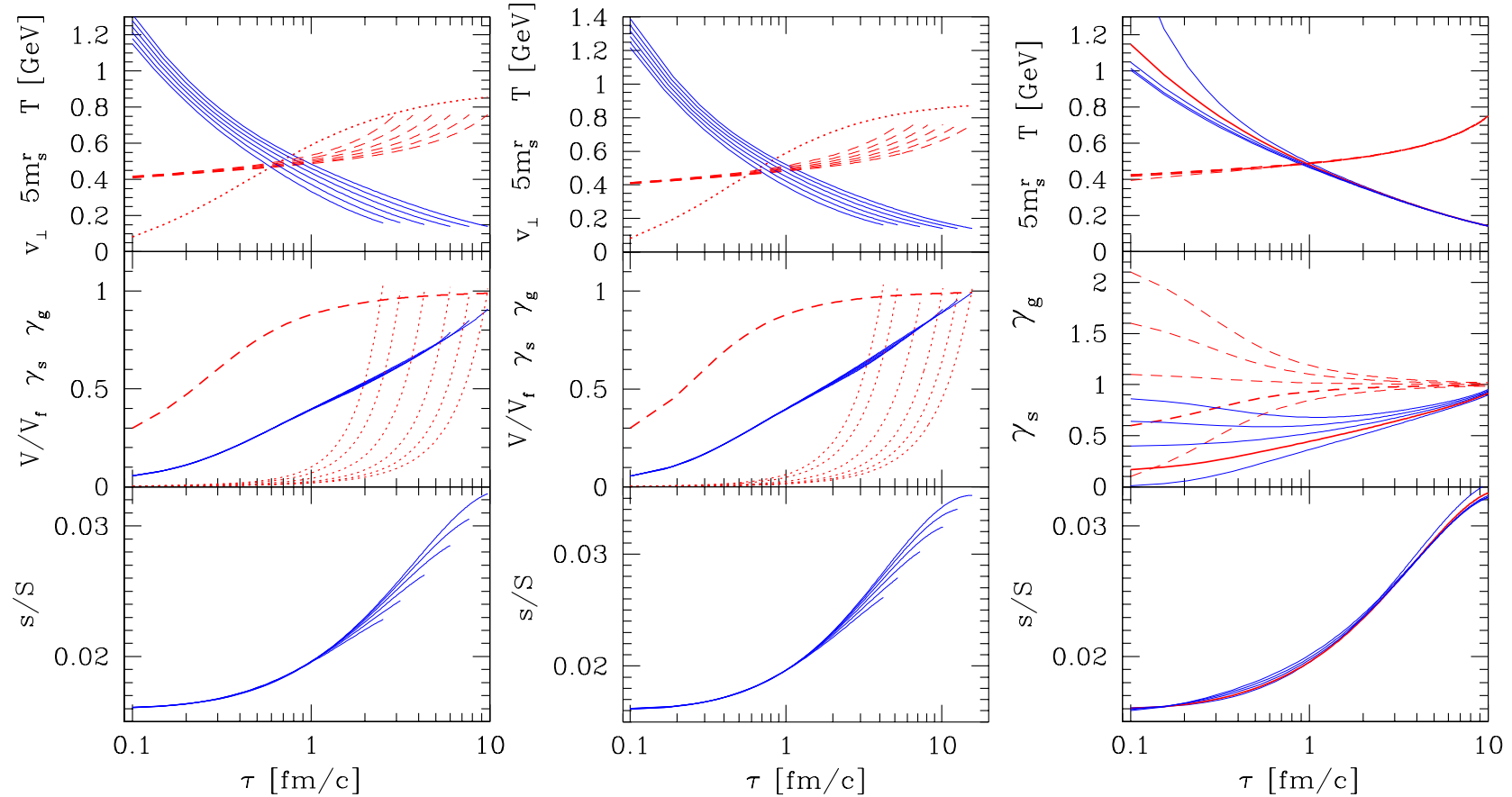
Early time behavior  $\gamma_G(\tau)$  and  $v(\tau)$  can be shown to be of minimal relevance. Strangeness looks back at times  $\tau \simeq 2 - 3$  fm. Beyond, for yet earlier  $\tau$  there is little, if any, memory.

## Understanding $s/S$ and $\gamma_s$ at RHIC



**The two left panels:** Comparison of the two transverse expansion models, bulk expansion (left), and wedge expansion. Different lines correspond to different centralities. **On right: study of the influence of the initial density of partons.** Top panel: temperature  $T$ , running mass  $m_s^r$ , dotted: the assumed profile of  $v_{\perp}(\tau)$ , the transverse expansion velocity; middle panel: dashed assumed  $\gamma_g(\tau)$ , dotted the assumed normalized  $dV/dy(\tau)$  normalized by the freeze-out value. Solid line(s): resulting  $\gamma_s$  for different centralities coincide; and bottom panel: resulting  $s/S$  for different centralities, with  $R_0$  stepped down for each line by factor 1.4. The end points at maximum  $\tau$  allow to find corresponding centrality curves. Initial temperatures change slightly to accommodate an observed change in  $dS/dy|_f$  beyond participant scaling. **Lifespan of system for most central reactions consistently  $\tau_f = 7 \pm 1$  fm. Freeze-out condition at  $T_f = 140$  MeV (higher  $T_f$  implies proportionally shorter  $\tau_f$ ).**

## What this means for LHC



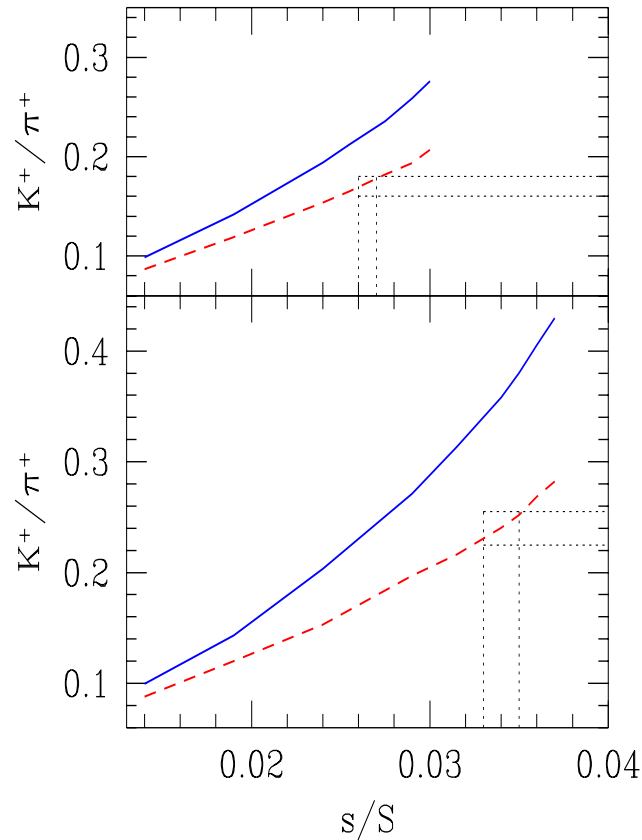
**The two left panels:** Comparison of the two transverse expansion models, bulk expansion (left), and wedge expansion. Different lines correspond to different centralities. **On right:** study of the influence of the initial density of partons.

**Notable LHC differences to RHIC:** (we assumed  $dS/dy|_{\text{LHC}} = 4dS/dy|_{\text{RHIC}}$ )

- There is a significantly longer expansion time to the freeze-out condition (factor 2).
- There is a 20% growth in  $s/S$  implying corresponding growth in  $K/\pi$ . More generally, there is a steady growth of  $s/S$  and  $\gamma_s$  with  $\ln dS/dy$ .
- There is a significant increase in initial temperature to accommodate increased entropy density.

Reconsider thermal charm production:

## How much enhancement in from RHIC to LHC $K/\pi$ ?



$K^+/\pi^+$  ratio as function of attained specific strangeness at freeze-out,  $s/S$ . Solid lines bare yields, dashed lines after all weak decays have diluted the pion yields. Top for RHIC and bottom for LHC physics environment. An increase by about 40% is predicted from  $K^+/\pi^+ = 0.17$  at RHIC to  $K^+/\pi^+ = 0.24$  at LHC. If LHC is subject to donut-expansion, increase more significant.

•

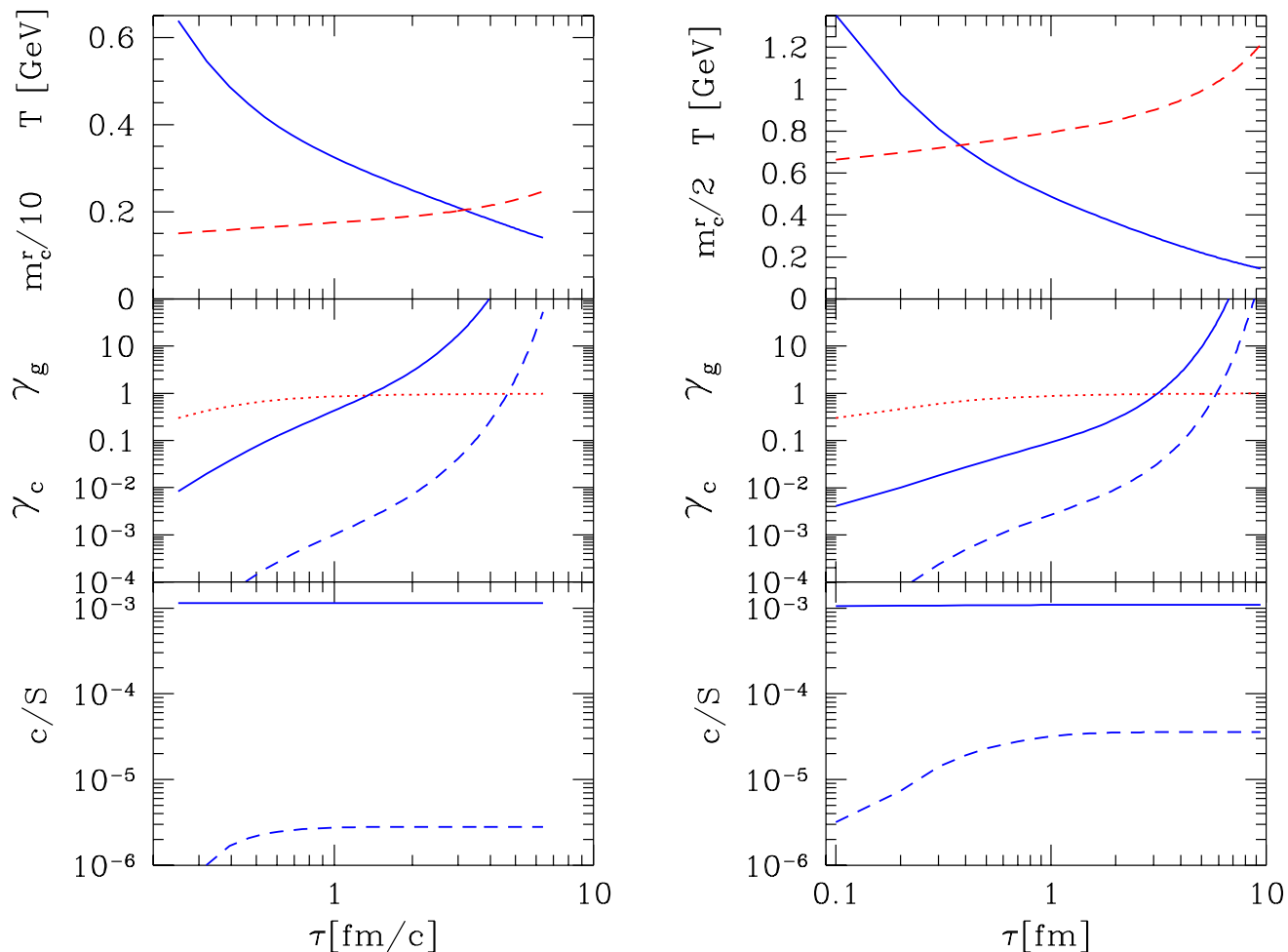
## 5. Implications for Charm at RHIC and LHC

First we look at thermal charm yield: guaranteed to be thermalized distribution at central rapidity

Next: statistical hadronization on rapidly expanding strangeness oversaturated system, evaluating all specific

$$\frac{\text{charmed hadron yields}}{\text{all charm (bottom) yield}}$$

## Thermal charm at LHC - comparison with direct charm production



Left RHIC and right LHC: Top panel: Solid lines  $T$ , dashed lines, running  $m_c$  (scaled with 10 for RHIC on left and with 2 on right for LHC); middle panel: Dotted line  $\gamma_g$ , solid lines total charm  $\gamma_c$ , dashed lines  $\gamma_c$  corresponding to thermal charm production; and bottom panel: specific charm yield per entropy, solid lines for all charm, and dashed lines for thermally produced charm.

**Thermal charm production alone exceeds significantly chemical equilibrium!**

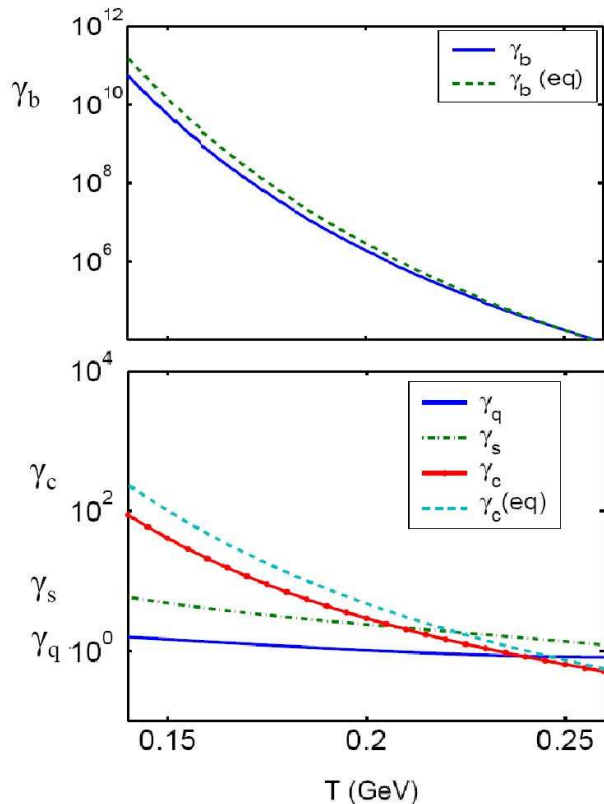
Direct production yield (to see assumed values multiply with  $dS/dy = 5000$  on left (RHIC) and  $=20,000$  on right (LHC)) remains significantly (300 at RHIC and 60 times at LHC) above thermal production (compare lines in bottom panel).

## Charm chemistry in presence of high $s/S$

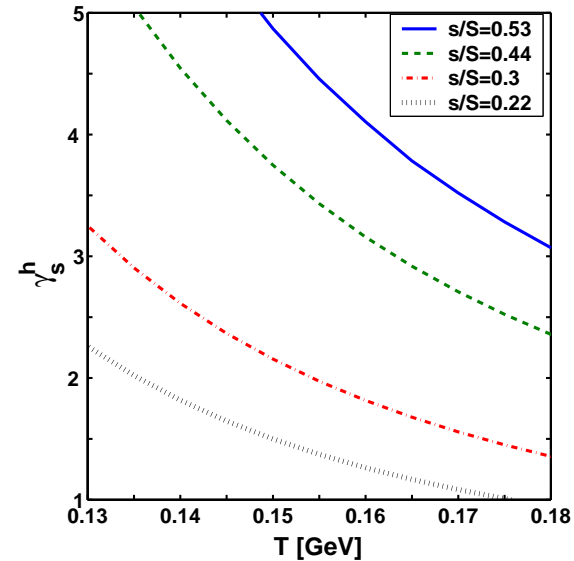
Recombination hadronization of charm has to be considered at a given  $s$  and  $S$  created in the dynamics of RHIC collision rather than for prescribed statistical yields. Charm distribution among particles according to:

$$\frac{dN_c}{dy} = \frac{dV}{dy} \left[ \gamma_c^h n_{\text{open}}^c + \gamma_c^{h2} (n_{\text{hidden}}^c + 2\gamma_q^h n_{ccq}^{\text{eq}} + 2\gamma_s^h n_{ccs}^{\text{eq}}) \right];$$

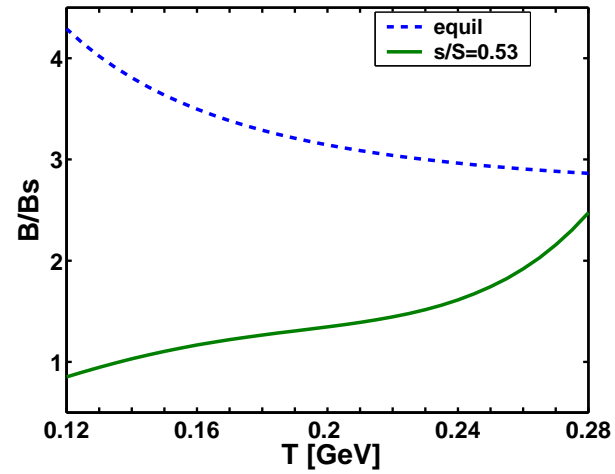
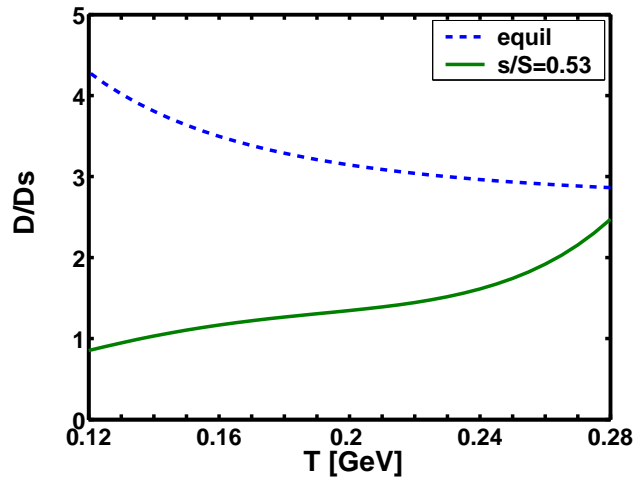
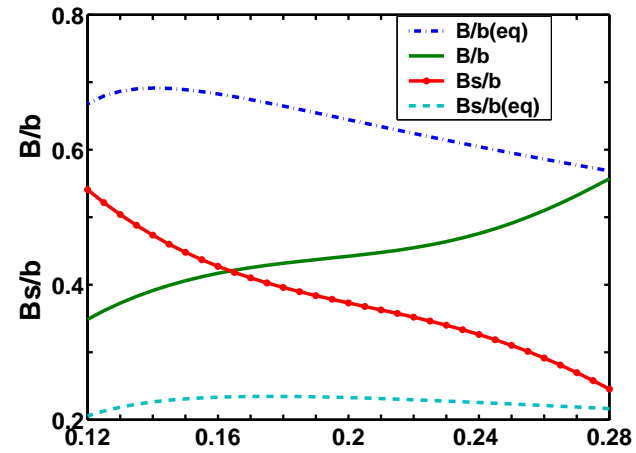
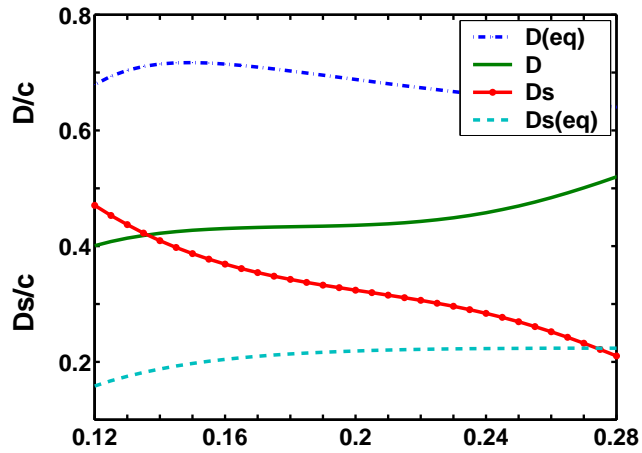
$$n_{\text{open}}^c = \gamma_q^h n_D^{\text{eq}} + \gamma_s^h n_{Ds}^{\text{eq}} + \gamma_q^{h2} n_{qqc}^{\text{eq}} + \gamma_s^h \gamma_q^h n_{sqc}^{\text{eq}} + \gamma_s^{h2} n_{ssc}^{\text{eq}}; \quad n_{\text{hidden}}^c = \gamma_c^{h2} n_{cc}^{\text{eq}}$$



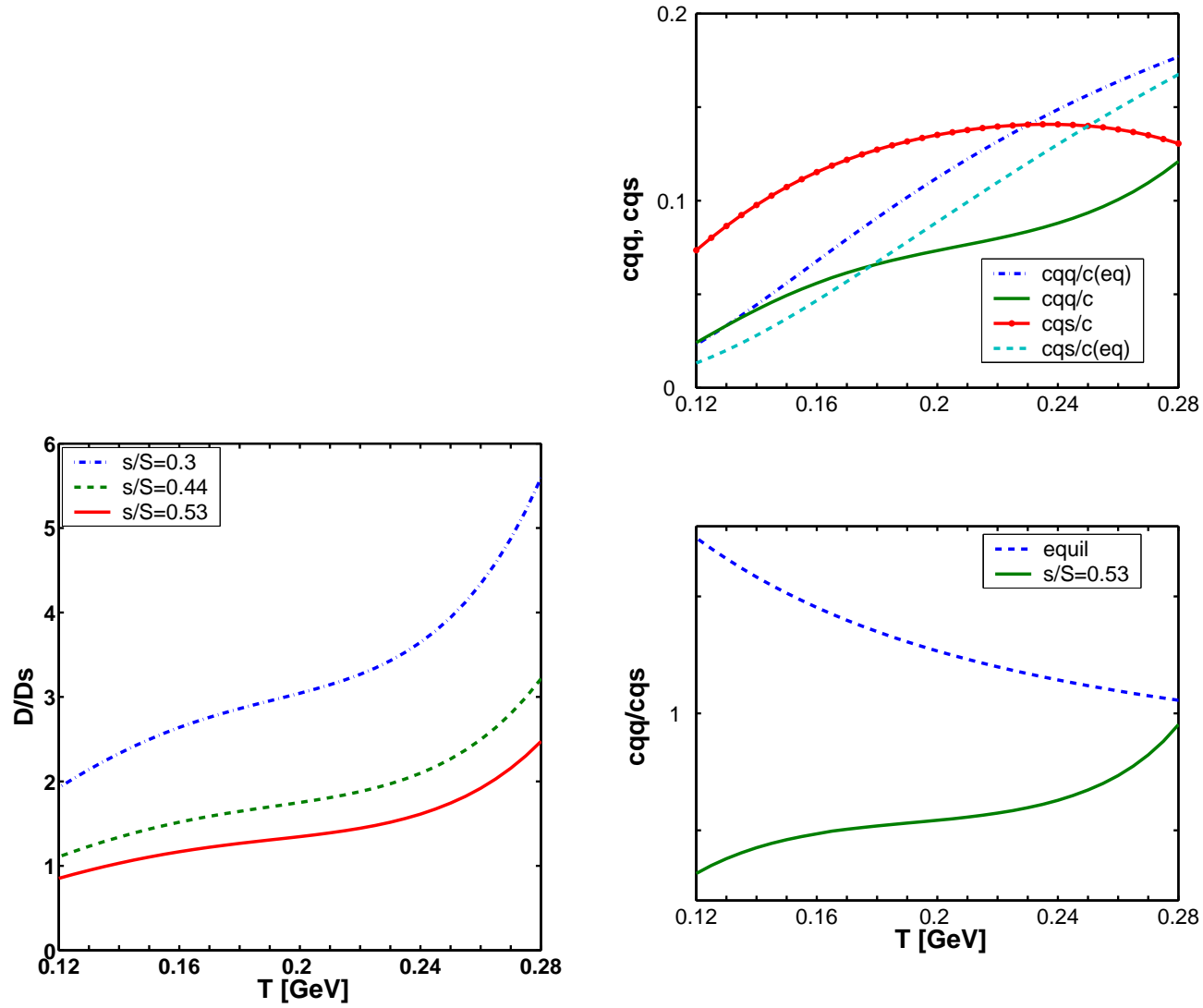
For  $db/dy = 1$ ,  $dc/dy = 10$ ,  $ds/dy = 650$  and  $dS/dy = 12,000$  (only 2.5 times RHIC) the hadron occupancies were obtained (equilibrium values for  $\gamma_i^{\text{QGP}} = 1$  for freeze-out at  $T$ ).



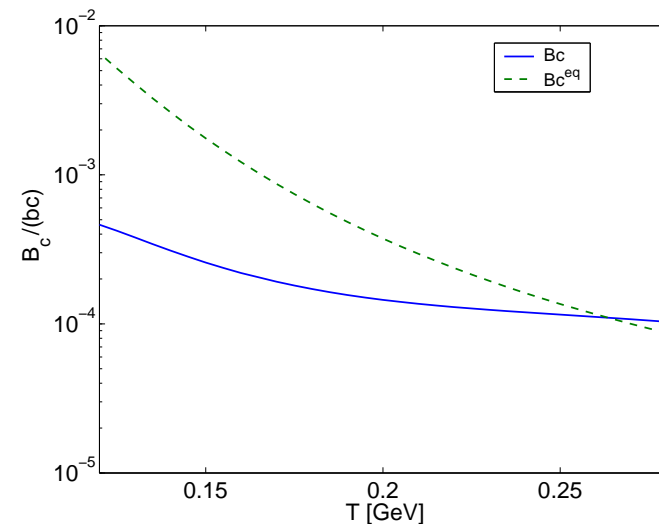
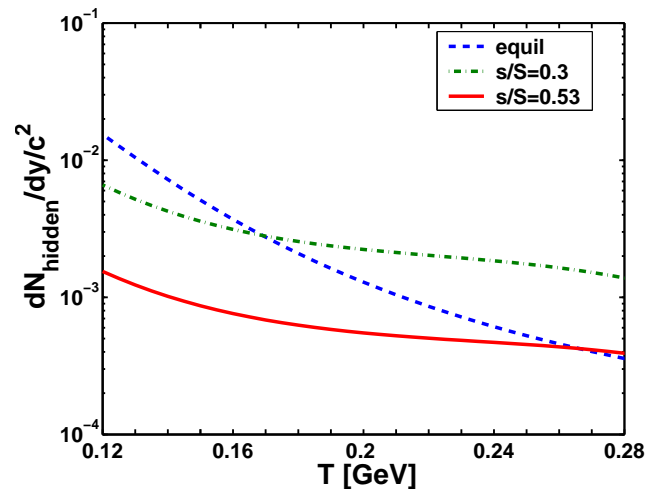
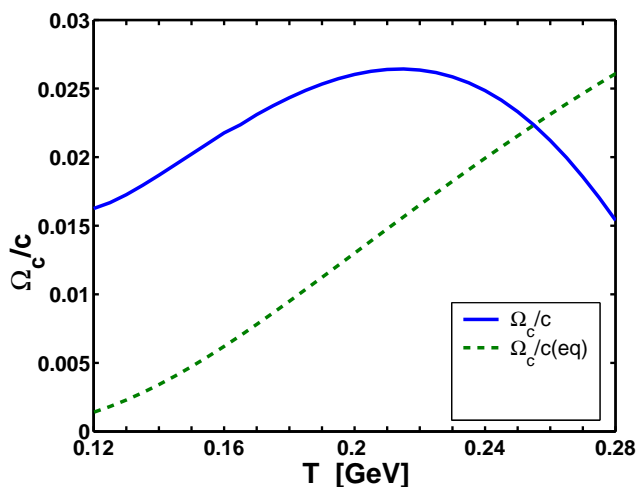
## Yields of $D$ , $D_s$ and $B$ , $B_s$ at $s/S = 0.053$



## Yields of $D$ , $D_s$ and c-baryons at variable $s/S$



## Yields of charmonium, css-baryons and $B_c$



Further work on heavy flavor chemistry on the way. Return now to discuss relevance of understanding of strangeness at LHC and phase transition dynamics.

## 6. Conclusions

- There is ample evidence for CHEMICAL equilibration of the QGP at freeze-out at RHIC and for fast hadronization. Hadron abundances are controlled by prevailing valence quark yields and are not in chemical equilibrium;
- Description of RHIC-200 results for  $K$ ,  $\phi$ ,  $K^*$  and nonstrange hadrons predicts precisely the strange baryon and antibaryon yields;
- Physical properties at Freeze-out such as  $E/TS, E/b$  can be extrapolated more easily across energy and allow prediction of LHC particle yields but strangeness content a parameter;
- QCD kinetic model tuned to describe strangeness at RHIC, predicts specific enhancement at LHC which is well within the naive expectations.  $K/\pi$  rises by 40%;
- Thermal charm (aside of direct charm) is present, produced in thermal glue fusion;
- Charmed strange baryons enhanced, impact multicharm hadron yields, charmonium reduced.